IOP Conf. Series: Journal of Physics: Conf. Series **1487** (2020) 012046 doi:10.1088/1742-6596/1487/1/012046

Variable Parameters Stiffness Identification and Modeling for Positional Compensation of Industrial Robots

Jiachen Jiao, Wei Tian*, Lin Zhang, Bo Li and Junshan Hu

College of Mechanical and Electrical Engineering, Nanjing University of Aeronautics and Astronautics, Nanjing 210016

*Corresponding author's E-mail address: tw_nj@nuaa.edu.cn

Abstract. Due to the weak stiffness of robot structure, the positional accuracy of industrial robots under load can hardly meet the application requirements of high-precision machining. Predicting and compensating errors by accurate stiffness modeling is an effective method to improve robot positional accuracy. Existing stiffness modeling methods use theoretical kinematic parameters and approximate the joint stiffness to a fixed value, so that the modeling accuracy is poor. Thus, this paper proposes a regular sampling point selection method by space gridding. Then, combining Levenberg-Marquardt kinematics parameter calibration and static joint stiffness identification methods, a comprehensive identification method is proposed to achieve simultaneous identifying of robot kinematics and stiffness parameters. Next, a variable parameter stiffness model could be established, according to the identification results in different workspaces. Finally, a model-based error prediction and compensation method is put forward through online sensing of external load. The error compensation is performed on a KR500 robot, and experimental results verified that the average value of absolute positional errors caused by external load, could be reduced by 44.61%, compared with the traditional compensation method.

1. Introduction

In recent years, the application of industrial robots as a machining carrier has considerably increased in automated manufacturing, because of the advantages of high task flexibility, high intelligence, low cost and low space requirement [1-3]. However, due to its structural characteristics, the positional accuracy and structural stiffness of industrial robots are much lower than those of traditional NC machines, which seriously affect their applications in high-value-added products manufacturing [4, 5]. An effective solution is to predict and compensate the positional error on the basis of robot stiffness model. Obviously, accurate stiffness identification and modeling of industrial robot is necessary to achieve precise positional control of robot under load.

There have been a lot of theoretical and experimental researches on the robot stiffness characteristics and modeling methods. Adele et al. built the mapping relationship between the stiffness matrices of the joint space and Cartesian space under the assumption of link rigidity [6]. Dumas et al. found that more than more than 70% of the deformation comes from the robot joint, and the Cartesian stiffness matrix of the robot can be solved by establishing its kinematic model and identifying its joint stiffness matrix [7]. Klimchik et al. coupled the influence of the gravity of the connecting rod on the robot stiffness, and further improved the accuracy of stiffness modeling. Furthermore, the compensation methods of positional error, which caused by processing load, have been extensively

researched based on robot stiffness mode [8]. Zaeh et al. realized compensation of milling path-deviation by robot joint stiffness identification and model-based fuzzy controller [9]. Slavkovic raised an off-line tool path modification method to compensate cutting force-induced errors in robotic machining [10].

Traditional robot stiffness modeling methods are proposed on the basis of the hypothesis that the connecting rods are rigid and each joint is an elastic rotating axis. Conveniently, the Cartesian stiffness model could be built through the combination of kinematic model and joint stiffness. However, there are some drawbacks of these methods. Firstly, theoretical kinematics parameters cannot truly reflect the structure attribute of robot because of the error of manufacturing and assembly. Secondly, the torsional stiffness of motor and reducer, and the gravity center of the connecting rod change with robot configuration. Thirdly, different robot sampling configurations lead to different identification results of joint stiffness. For these reasons, theoretical kinematics parameters and fixed joint stiffness cannot meet the accuracy of robot stiffness modeling. Moreover, the precise prediction and compensation of positional error under external load cannot be achieved.

This paper proposed a variable stiffness modeling method of industrial robots, and the stiffness characteristics of robots in different work spaces can be accurately characterized. In Section 2, the modeling methods of robotic kinematic and stiffness error are described. Section 3 proposes a regular sampling point planning method based on space grid, and a variable parameter identification method of kinematics and stiffness parameters is put forward. A model-based positional error compensation method is proposed in section 4. The results of the experimental verification are shown in Section 5. Finally, the paper is concluded in Section 6.

2. Modeling of robot kinematics and stiffness error

2.1. Modeling of kinematics error

Kinematic model is the foundation of robot stiffness identification and modeling. The link frames and theoretical kinematics model of KUKA KR500 industrial robot can be established through Denavit-Hartenberg (D-H) model method, as shown in figure 1 [11].

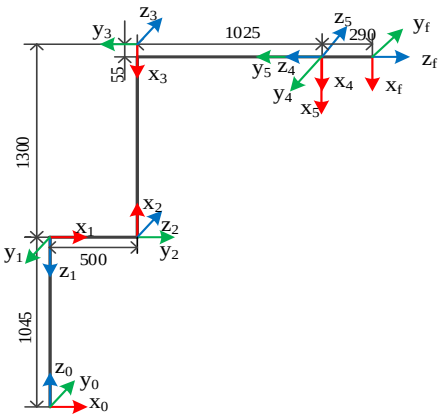

Figure 1. KUKA KR500 robot kinematic model.

According to the robot kinematic model, the transformation relationship between the robot positional error and the parameters error of each link can be obtained; conversely, the parameters error of each link of the robot can be solved iteratively according to the positional error, and the actual kinematic parameters of the robot can be calibrated.

Define the position error of *i*-th target point without external load as Δp_i:

$$\Delta p_i = \frac{\partial p_i}{\partial a}\Delta a + \frac{\partial p_i}{\partial \alpha}\Delta \alpha + \frac{\partial p_i}{\partial d}\Delta d + \frac{\partial p_i}{\partial \theta}\Delta \theta = J_i \Delta X, \Delta X = \begin{bmatrix} \Delta a & \Delta \alpha & \Delta d & \Delta \theta \end{bmatrix}^{\mathrm{T}} \quad (1)$$

where a is the link length, α the link torsion angle, θ the joint angle, and d the offset of adjacent links, respectively, and J_i is the Jacobian matrix. For a 6-DOF manipulator, each of the parameter error vectors (i.e. $\Delta a, \Delta\alpha, \Delta d, \Delta\theta$) has 6 elements.

If m sampling points were measured during kinematics calibration:

$$\begin{bmatrix} \Delta p_1 \\ \Delta p_2 \\ \mathrm{M} \\ \Delta p_m \end{bmatrix} = \begin{bmatrix} \frac{\partial p_1}{\partial a} & \frac{\partial p_1}{\partial \alpha} & \frac{\partial p_1}{\partial d} & \frac{\partial p_1}{\partial \theta} \\ \frac{\partial p_2}{\partial a} & \frac{\partial p_2}{\partial \alpha} & \frac{\partial p_2}{\partial d} & \frac{\partial p_2}{\partial \theta} \\ \mathrm{M} & \mathrm{M} & \mathrm{M} & \mathrm{M} \\ \frac{\partial p_m}{\partial a} & \frac{\partial p_m}{\partial \alpha} & \frac{\partial p_m}{\partial d} & \frac{\partial p_m}{\partial \theta} \end{bmatrix} \begin{bmatrix} \Delta a \\ \Delta \alpha \\ \Delta d \\ \Delta \theta \end{bmatrix} = \begin{bmatrix} J_1 \\ J_2 \\ \mathrm{M} \\ J_m \end{bmatrix} \Delta X \tag{2}$$

The kinematic parameter error calibration could be seen as a solution of linear equations. The Levenberg-Marquardt (L-M) algorithm can be used for iterative computation. The k-step iterative procedure is as follows:

(1) Calculate $J(\mathrm{X}_k)$ according to the D-H parameters of the robot.

(2) Calculate the error of D-H parameters ΔX_k on account of the formula:

$$\Delta X_k = -\left[J\left(X_k\right)^{\mathrm{T}} J\left(X_k\right) + \mu_k I \right]^{-1} J\left(X_k\right)^{\mathrm{T}} \Delta p(X_k) \tag{3}$$

where I is a unit matrix; X_k is the parameter error in the k-th iteration; μ_k is the damping coefficient which could be obtained by:

$$\begin{cases} \mu_0 = 0.001 \\ \mu_{k+1} = \begin{cases} 0.001\delta & \text{if } \left\|\Delta p\left(\boldsymbol{X}_{k+1}\right)\right\| \geq \left\|\Delta p\left(\boldsymbol{X}_k\right)\right\| \\ 0.001/\delta & \text{if } \left\|\Delta p\left(\boldsymbol{X}_{k+1}\right)\right\| < \left\|\Delta p\left(\boldsymbol{X}_k\right)\right\| \end{cases} \\ 2.5 < \delta < 10 \end{cases} \tag{4}$$

(3) Update D-H parameters of the robot by $X_{k+1} = X_k + \Delta X_k$ and update iterations by $k = k + 1$.

Repeat the above steps to get the error of each link parameter of the robot, and modified kinematics model could be obtained. The modified kinematic model can be used as the basis for accurate identification of stiffness.

2.2. Modeling of stiffness error

For six-revolute joint serial robots, the mapping relationship between the joint and Cartesian stiffness matrixes could be represented by using conservative congruence transformation as:

$$K = J^{-T} K_\theta J^{-1} \tag{5}$$

$$K_\theta = diag\left(k_{\theta_1}, k_{\theta_2}, k_{\theta_3}, k_{\theta_4}, k_{\theta_5}, k_{\theta_6}\right) \tag{6}$$

where J is the Jacobian matrix related to the robot configuration directly; K and K_θ are the joint and Cartesian stiffness matrixes respectively; $k_{\theta i}$ is the stiffness of i-th joint. The above formula is called the traditional static stiffness model, indicating that the robot stiffness depends on the joint stiffness and the configuration [12].

The Cartesian stiffness matrix K could be divided into four 3×3 matrixes according to the different dimensions of factors among stiffness matrix, which could be described as

$$\begin{bmatrix} f \\ m \end{bmatrix} = \begin{bmatrix} K_{fd} & K_{f\delta} \\ K_{md} & K_{m\delta} \end{bmatrix} \begin{bmatrix} d \\ \delta \end{bmatrix} \tag{7}$$

where f and m are the force and torque applied on end effector; d and δ are the translational and rotational displacements of end effector respectively; K_{fd}, $K_{f\delta}$, K_{md}, $K_{m\delta}$ are the associated stiffness coefficients. In robot cutting tasks, such as drilling and milling, the influence of rotational

displacement on robot positional accuracy can be neglected. Consequently, the relationship of f and d could be shown as below:

$$f = K_{fd} d \tag{8}$$

Then the positional errors caused by external load can be written as:

$$d = K_{fd}^{-1} f = D\left(JK_{\theta}^{-1} J^{T}\right) f \tag{9}$$

where D is a function to pick up the first three columns elements of the first three lines of a given matrix, and the formula can be used to predict the robot positional error under external load [13].

3. Variable parameter identification based on space gridding

Different robot sampling configuration leads to different positional error, no matter in no-load or load state. On the one hand, different configuration results in different gravity center of robot structure and connecting rod deformations, which influence the identification results of kinematics parameters and joint stiffness. On the other hand, the joint stiffness and rotation angle of each joint are interrelated to each other, due to the complex transmission structure, including motor and reducer mainly [14, 15]. Thus, fixed parameters cannot satisfy the accuracy requirement of robot modeling very well. In view of the similar robot configurations in close work spaces, a variable parameter identification method is extremely essential to reduce the influence of the configuration on robot stiffness modeling.

3.1. Space gridding principle analysis

If the robot configuration were determined, the parameter error in each joint can be determined. Define ΔP_1 as the error of kinematics parameters in a given configuration, ΔP_2 as the error of kinematics parameters in a close configuration:

$$E = \left|\Delta P_1 - \Delta P_2\right| < \xi, \quad \Delta\theta \to 0 \tag{10}$$

where $\triangle\theta$ is the variation of joint angles in two configurations, E is the absolute value of the difference. As $\triangle\theta$ tends to zero, a positive number ξ which approaches zero can always be found to satisfy $E<\xi$.

Similarly, define $K_{\theta 1}$ as the joint stiffness of a joint in a given angle, $K_{\theta 2}$ as the joint stiffness of the joint in a similar angle:

$$E' = \left|K_{\theta 1} - K_{\theta 2}\right| < \xi', \quad \Delta\theta \to 0 \tag{11}$$

where E' is the absolute value of the difference. As $\triangle\theta$ tends to zero, a positive number ξ' which approaches zero can always be found to satisfy $E'<\xi'$.

Accordingly, when robot configuration changes a little, namely the position and posture of end effector changes a little, the kinematics parameter and the stiffness value of each joint can be considered to be highly similar.

The above analysis indicates that workspace can be divided and parameters in a subspace can be approximately seen as constant values. Since regular shape can greatly improve algorithm efficiency, the workspace could be divided into small cubic grids as shown in figure 2. Accordingly, eight vertices and the center point of each space grid are selected as sampling points. Therefore, a total of nine sampling points are used to identify robot kinematics and stiffness parameters in a certain grid space, as shown in Tag 1 to Tag 9 in figure 2.

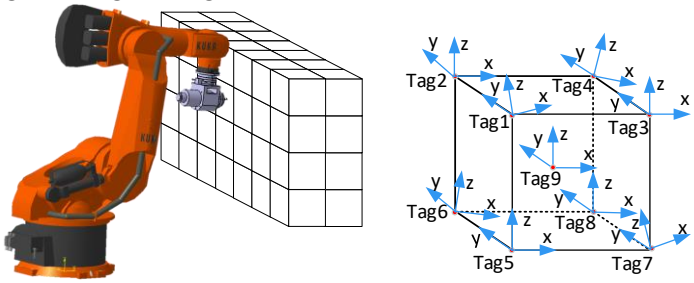

Figure 2. Work space gridding and sampling.

3.2. Variable parameter identification

Combing the space gridding sampling and traditional parameter identification methods, a variable parameter stiffness identification method can be presented. Sampling points of identification experiments could be decided based on space grids. The actual kinematics parameters which satisfy different workspaces are defined as:

$$X(j)=\left[a(j) \quad \alpha(j) \quad d(j) \quad \theta(j)\right]^{\mathrm{T}} \tag{12}$$

where j is the sequence number of target grid space, and $\mathrm{X}(j)$ is the kinematics parameters when robot target position is in corresponding grid space. Then, the Jacobian matrix in different work spaces could be revised based on corresponding kinematics parameters. Accordingly, the joint stiffness which suits different workspaces can be accurately calculated and described as

$$K_{\theta}(j)=diag\left(k_{\theta_1}(j)\mathrm{L}\ k_{\theta_6}(j)\right) \tag{13}$$

The steps of variable parameter stiffness identification and modeling method could be shown as follow:

(1) Divide the whole workspace into a series of cubic grids according to the given side length.

(2) Choose the theoretical coordinates of the nine samplings of a grid space as sampling positions. Define the initial posture of end effector in each sample point, and the initial robot configuration could be obtained.

(3) Rotate the Tool candidate around a processing axis and obtain new sampling configurations in each position.

(4) Control the robot move to the target configurations without loading, the actual kinematics parameters could be identified by dealing with theoretical position and actual positions. Modified Jacobian matrix could be built by identification results.

(5) Control the robot move to the target configurations with loading, the robot stiffness could be identified by measuring actual positions before and after loading.

(6) Repeat the fourth step to fifth step to obtain the joint stiffness in different task spaces.

(7) Finally, establish the robot stiffness model of whole work space.

The workflow of identification method can be shown as figure 3.

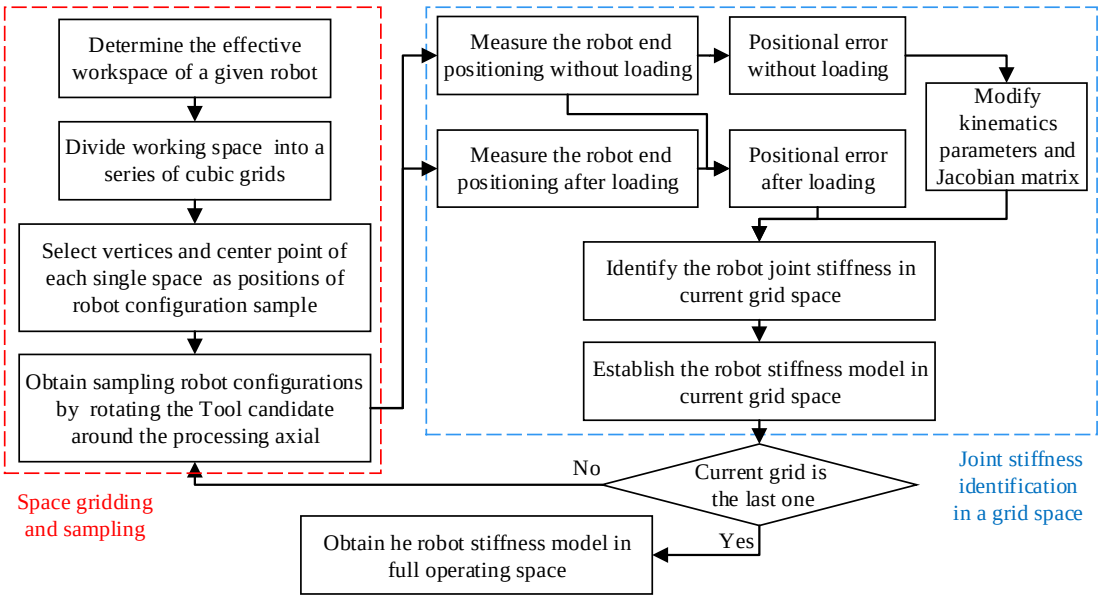

Figure 3. Identification flowchart.

4. Model-based robot positional compensation

The positional error of target points in different subspaces could be estimated based on the variable parameters stiffness model and on-line measurement of robot load. Compensation of robot positional

errors caused by external load, can be performed by modifying the numerical control commands of robot, which includes the following steps:

(1) Plan space grids and generate sampling points in off-line programming (OLP) software, kinematics parameters and joint stiffness in different grids can be identified by identification method proposed in Section 3.

(2) Extract the positions of target points from robot control commands and plan corresponding robot configurations in OLP software. Define the position coordinates of *i*-th target point:

$$P(i) = \begin{bmatrix} P_x(i) & P_y(i) & P_z(i) \end{bmatrix} \tag{14}$$

(3) Estimate the located grid space of given target position and obtain the suitable robot joint stiffness.

(4) Measure the load applied to the end effector by force transducer during robot tasks. Define the external load of *i*-th target point:

$$F(i) = \begin{bmatrix} F_x(i) & F_y(i) & F_z(i) \end{bmatrix}^{\mathrm{T}} \tag{15}$$

(5) Calculate the load-induced positional errors:

$$\Delta P(i) = \begin{bmatrix} \Delta P_x(i) & \Delta P_y(i) & \Delta P_z(i) \end{bmatrix}^T = D\left(J(i) K_\theta^{-1}(i) J^{\mathrm{T}}(i) \right) F(i) \tag{16}$$

where $\Delta P_x(i)$, $\Delta P_y(i)$ and $\Delta P_z(i)$ are predicted positional errors of given target position along the directions of *x*, *y* and z axis, $K_\theta^{-1}(i)$ is the robot compliance matrix, and $J(i)$ is the Jacobian matrix of the *i*-th target position.

(6) Compensate the positional error through the following equation:

$$P^{'}(i) = P(i) - \Delta P(i) \tag{17}$$

where $P^{'}(i)$ is the modified position coordinate, and the revised coordinate could be loaded as control commands to achieve high-precision robot positional control.

5. Experimental results and discussion

5.1. Experimental setup

An experimental platform and coordinate systems were built to verify the presented method, as shown in figure 4. A KR500 (KUKA Inc.) industrial robot was used as the motion carrier. An IP60 Omega160 (ATI Inc.) six-dimensional force transducer, which was mounted on the flange, was used to measure the external load. The end effector was installed under the force transducer and a 50 kg external load was used to generate desired elastic deflections. The robot positional errors were measured by a laser tracker (API Inc.) through a spherically mounted retroreflector (SMR), which was installed on the end effector.

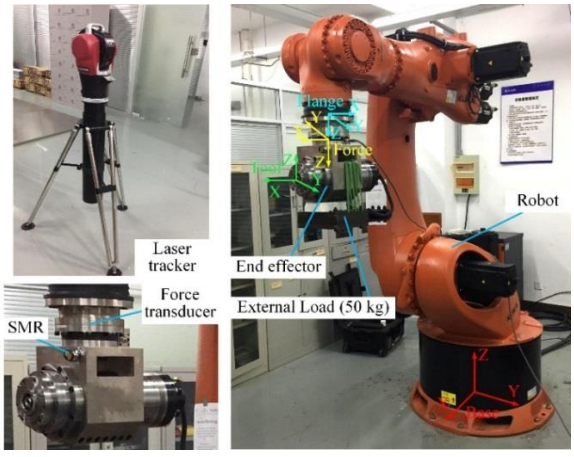

Figure 4. Experimental system.

5.2. Experiment of variable parameter stiffness identification

A 1200 mm × 600 mm × 600 mm workspace was planned as the robot calibration space in the experiment. The different side lengths of 600 mm, 300 mm and 150 mm were selected to investigate the influence of grid size on identification results, as shown in figure 5.

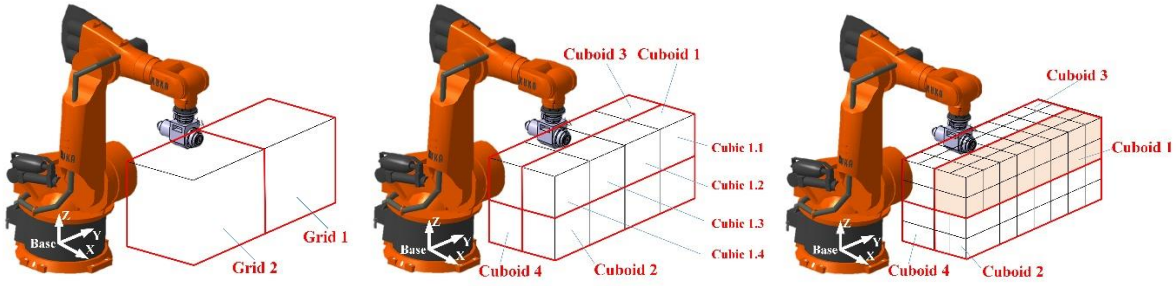

Figure 5. Space division with different side lengths of grid.

On this basis, the theoretical coordinates and the initial configuration in each sample point could be planned. Rotate the end effector around the y axis of Tool candidate system with -10 ° and 10 °, new robot configurations in given position were generated. Besides, deformations without loading and deformations caused by external load were measured respectively through laser tracker in the base coordinate system. External loads were measured through force transducer in the force coordinate system. Accordingly, actual kinematics parameters and stiffness of each robot joint in different grid spaces could be identified. Specific situations are presented as follows.

Selecting eight vertices and the center point of the whole calibration space as sampling points, stiffness of each robot joint without modification of kinematics parameters could be identified as

$$K_\theta = \mathrm{diag}(1.49\times10^{10}, 6.03\times10^{9}, 5.56\times10^{9}, 3.70\times10^{8}, 2.52\times10^{8}, 4.53\times10^{8}) \ \mathrm{Nmm/rad} \quad (18)$$

The stiffness of each robot joint with modified kinematics parameters could be identified as

$$K_\theta = \mathrm{diag}(1.56\times10^{10}, 6.12\times10^{9}, 5.83\times10^{9}, 4.59\times10^{8}, 2.19\times10^{8}, 4.79\times10^{8}) \ \mathrm{Nmm/rad} \quad (19)$$

The identification results have changed compared to those before kinematics parameters modification.

Choosing 600 mm as the side length of the cubic grid, the robot calibration space was divided into 2 symmetrical cubic grids. Then, joint stiffness in two grids could be identified after modification of kinematics parameters, the identification results could be shown as

$$K_{\theta G1} = \mathrm{diag}(1.48\times10^{10}, 5.58\times10^{9}, 6.81\times10^{9}, 3.68\times10^{8}, 1.40\times10^{8}, 2.06\times10^{8}) \ \mathrm{Nmm/rad} \quad (20)$$

$$K_{\theta G2} = \mathrm{diag}(1.49\times10^{10}, 6.81\times10^{9}, 4.81\times10^{9}, 2.28\times10^{8}, 3.99\times10^{8}, 1.65\times10^{8}) \ \mathrm{Nmm/rad} \quad (21)$$

where $K_{\theta G1}$ and $K_{\theta G2}$ are diagonal matrixes of joint stiffness in Grid 1 and Grid 2 spaces as shown in figure 5. The stiffness of each joint changes slightly in these two spaces.

The robot calibration space was divided into 16 cubic grids when choosing 300 mm as the side length of the cubic grid. The joint stiffness in 16 grids could be identified after modification of kinematics parameters as shown in table 1.

Table 1. The stiffness of third joint in 16 grid spaces.

$K_{\theta i}$ (Nmm/ rad)	$K_{\theta 1}$	$K_{\theta 2}$	$K_{\theta 3}$	$K_{\theta 4}$	$K_{\theta 5}$	$K_{\theta 6}$
Cubic 1.1	1.06×10^{10}	5.56×10^{9}	6.40×10^{9}	3.24×10^{8}	1.31×10^{8}	2.04×10^{8}
Cubic 1.2	6.85×10^{9}	5.59×10^{9}	6.29×10^{9}	1.88×10^{8}	9.23×10^{7}	1.26×10^{8}
Cubic 1.3	8.24×10^{9}	5.88×10^{9}	6.04×10^{9}	1.68×10^{8}	7.30×10^{7}	1.20×10^{8}
Cubic 1.4	1.01×10^{10}	7.51×10^{9}	4.29×10^{9}	1.83×10^{8}	2.88×10^{8}	1.83×10^{8}
Cubic 2.1	1.82×10^{9}	5.36×10^{9}	6.80×10^{9}	6.27×10^{7}	1.17×10^{8}	6.27×10^{7}
Cubic 2.2	2.05×10^{9}	5.39×10^{9}	8.57×10^{9}	5.76×10^{7}	7.28×10^{7}	5.76×10^{7}
Cubic 2.3	2.51×10^{9}	5.48×10^{9}	9.24×10^{9}	5.64×10^{7}	5.07×10^{7}	5.64×10^{7}
Cubic 2.4	2.64×10^{9}	6.85×10^{9}	4.88×10^{9}	5.20×10^{7}	2.05×10^{8}	5.20×10^{7}

Cubic 3.1	6.95×10^{10}	5.04×10^{9}	6.36×10^{9}	7.06×10^{8}	1.42×10^{8}	4.74×10^{8}
Cubic 3.2	8.29×10^{9}	4.95×10^{9}	6.13×10^{9}	2.60×10^{8}	9.46×10^{7}	1.80×10^{8}
Cubic 3.3	1.06×10^{10}	5.42×10^{9}	5.46×10^{9}	2.34×10^{8}	1.10×10^{8}	2.07×10^{8}
Cubic 3.4	4.37×10^{9}	7.32×10^{9}	4.27×10^{9}	1.17×10^{8}	1.16×10^{9}	1.13×10^{8}
Cubic 4.1	2.70×10^{9}	4.50×10^{9}	7.49×10^{9}	1.22×10^{8}	1.28×10^{8}	7.33×10^{7}
Cubic 4.2	2.83×10^{9}	4.70×10^{9}	8.53×10^{9}	1.01×10^{8}	8.12×10^{7}	4.56×10^{7}
Cubic 4.3	2.64×10^{9}	5.13×10^{9}	7.38×10^{9}	7.62×10^{7}	8.11×10^{7}	3.60×10^{7}
Cubic 4.4	2.24×10^{9}	6.72×10^{9}	4.39×10^{9}	5.62×10^{7}	2.30×10^{8}	2.49×10^{7}

And so on, the joint stiffness in 128 grids could be identified.

Through above description, kinematics parameters modification or not influences the identification results of joint stiffness. Furthermore, the joint stiffness obviously changes in grid space of different sizes.

5.3. Experiment of robot positional compensation

In theory, no kinematic modification and larger grid space can result in lower accuracy of stiffness identification results. Thus, model-based compensation experiments were performed to test the actual effect of positional error compensation, and the application effect of variable parameters model of robot stiffness could be concurrently reflected.

Choosing one verification point randomly in each 150 mm × 150mm × 150 mm grid of calibration space, and 128 verification points were generated. Fixing an external load on the end effector to simulate the machining load, the positional errors of target points were predicted based on the measured load and the corresponding stiffness model. After that, the actual positional errors before and after compensating could be measured by executing commands before and after modification. The absolute positional errors could be calculated using the equation:

$$E(i)=\sqrt{\left(E_x(i)\right)^2+\left(E_y(i)\right)^2+\left(E_z(i)\right)^2} \tag{22}$$

where $E(i)$ is the absolute positional error of the i-th target position, $E_x(i)$, $E_y(i)$ and $E_z(i)$ are the positional errors on x, y and z axis respectively.

In order to researching the effect of kinematics parameters modification, the compensation experiments were conducted without space gridding. The positional error compensation results before and after modifying kinematic parameters were compared as shown in figure 6. After modifying kinematic parameters, the average value of robot absolute positional error was reduced from 0.1104 mm to 0.1049 mm. The experimental results show that the stiffness modeling accuracy is higher after kinematics parameters modification. Consequently, the identification of joint stiffness in each grid space was based on the modified kinematic parameters in subsequent experiments.

The compensation effect in different sizes of divided grid space could be shown as figure 7. The average value of absolute positional errors caused by external load was 0.2567 mm, and the maximum error was 0.3244 mm. Based on invariable joint stiffness, the average absolute positional error after compensation was reduced a certain extent to 0.1049 mm; the maximum error was 0.1434 mm. The average value of absolute positional errors was decreased to 0.0989 mm through grids with 600 mm side length, and the maximum error was 0.1434 mm. Dividing workspace into 16 grids and the positional accuracy could be raised further. The average absolute positional error was reduced to 0.0761 mm and the biggest error was 0.1129 mm. Finally, dividing the calibration space into 128 grids and the average value of absolute positional errors was cut down to 0.0581 mm and the biggest error was 0.0981 mm. The positional accuracy reached within 0.1 mm generally. Accordingly, the smaller grid size, the more accurate compensation results could be obtained. Compared with the traditional compensation method, whose joint stiffness is constant, the compensation effect with 128 grids raised by nearly 44.61%.

In summary, it can be proved that the joint stiffness varies indeed in different spaces. When the kinematics parameters and the joint stiffness change with work space, the robot stiffness model and

error prediction model could be better characterized. Hence, the error compensation method based on variable parameters can effectively improve positional accuracy of robot machining system under external load.

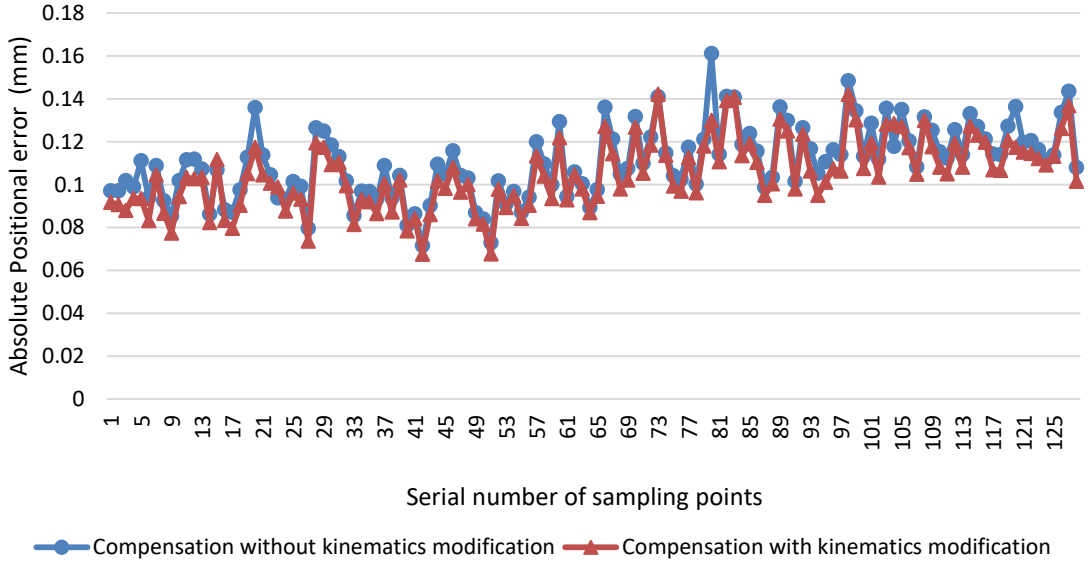

Figure 6. Compensation results with or without kinematics modification.

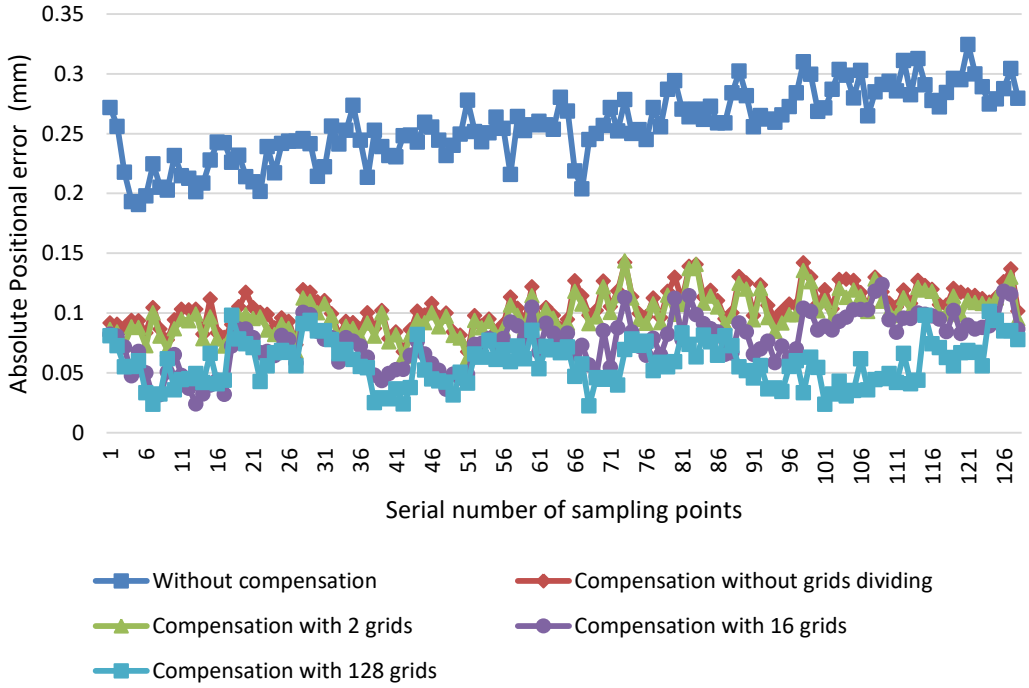

Figure 7. Absolute positional errors before and after compensation.

6. Conclusions

(1) This paper raised a regular sampling point selection method by space gridding.

(2) A robotic variable parameter stiffness modeling method is put forward, based on the identification of kinematics parameters and joint stiffness in different space grid.

(3) Combining force online perception method and variable parameter stiffness model, a positional error prediction and compensation method is built.

(4) Experiments of the stiffness identification and positional error compensation methods were performed on KUKA KR500 experimental system. Positional errors caused by external load could be reduced obviously, and the effectiveness of the modeling method was testified. In addition, a certain relationship exists between the compensation effect and the number of grids, which could be used for reference in future research.

(5) The method has good application value in high-precision machining tasks, such as robot drilling and milling.

Acknowledgments
This study was co-supported by National Natural Science Foundation of China (No. 51875287) and National Defense Basic Scientific Research Program of China (No. JCKY2018605C002).

References

[1] Song D, Kan Z, Wenhe L 2018 Stability of lateral vibration in robotic rotary ultrasonic drilling *International Journal of Mechanical Sciences*. S0020740318309664-
[2] Garnier S, Subrin K, Waiyagan K 2017 Modeling of Robotic Drilling *Procedia CIRP*. 58:416-421
[3] Zhou J, Nguyen H N, Kang H J 2014 Simultaneous identification of joint compliance and kinematic parameters of in-dustrial robots *International Journal of Precision Engineering and Manufacturing.* 15(11):2257-2264
[4] Guo Y, Dong H, Wang G, et al 2016 Vibration analysis and suppression in robotic boring process *International Journal of Machine Tools and Manufacture.* 101:102-110
[5] Abele E, Stefan Rothenbücher, Weigold M 2008 Cartesian compliance model for industrial robots using virtual joints *Production Engineering*. 2(3):339-343
[6] Abele E, Weigold M, Rothenbücher S 2007 Modeling and Identification of an Industrial Robot for Machining Applications *CIRP Annals - Manufacturing Technology*. 56(1):387-390
[7] Dumas C, Caro S, Garnier S, Furet B 2011 Joint stiffness identification of six-revolute industrial serial robots *Robotics and Computer-Integrated Manufacturing*. 27: 881–888.
[8] Klimchik A, Furet B, Stéphane Caro, et al 2015 Identification of the manipulator stiffness model parameters in industrial environment *Mechanism & Machine Theory.* 90:1-22
[9] Zaeh M F, Roesch O 2014 Improvement of the machining accuracy of milling robots *Production Engineering*. 8(6):737-744
[10] Slavkovic N R, Milutinovic D S, Glavonjic M M 2014 A method for off-line compensation of cutting force-induced errors in robotic machining by tool path modification *The International Journal of Advanced Manufacturing Technology*. 70(9-12):2083-2096
[11] Lin P D, Tsai I J 1996 The machining and on-line measurement of spatial cams on four-axis machine tools *International Journal of Machine Tools and Manufacture.* 1996, 36: 89-101
[12] Alici G, Shirinzadeh B 2005 Enhanced stiffness modeling, identification and characterization for robot manipulators *IEEE Transactions on Robotics*. 21(4):554-564
[13] Cordes M, Hintze W 2017 Offline simulation of path deviation due to joint compliance and hysteresis for robot machin-ing *The International Journal of Advanced Manufacturing Technology.* 90(1-4):1075-1083
[14] Yang K, Yang W, Cheng G, et al 2018 A new methodology for joint stiffness identification of heavy duty industrial robots with the counterbalancing system *Robotics and Computer-Integrated Manufacturing.* 53:58-71.
[15] Zeng Y, Tian W, Li D, et al 2017 An error-similarity-based robot positional accuracy improvement method for a robotic drilling and riveting system *The International Journal of Advanced Manufacturing Technology.* 88(9-12):2745-2755